CONF-9511130--1

UCRL-JC-120547
PREPRINT

Detecting Leaks in Hydrocarbon Storage Tanks Using Electrical Resistance Tomography

W. Daily
A. Ramirez
D. LaBrecque
A. Binley

This paper was prepared for submittal to
Frontiers 95
San Luis Obispo, CA
November 1995

April 3, 1995

Lawrence Livermore National Laboratory

DISTRIBUTION OF THIS DOCUMENT IS UNLIMITED

DISCLAIMER

Detecting Leaks in Hydrocarbon Storage Tanks Using Electrical Resistance Tomography

William Daily
Abelardo Ramirez
Lawrence Livermore National Laboratory
Livermore, CA 94550

and

Douglas LaBrecque
University of Arizona
Tucson, Arizona 85721

and

Andrew Binley
Lancaster University
Lancaster, England LA1 4YQ, UK

April 1995
rev.0

1. Introduction

Large volumes of hydrocarbons are stored worldwide in surface and underground tanks. It is well documented [1] that all too often these tanks are found to leak, resulting in not only a loss of stored inventory but, more importantly, contamination to soil and groundwater. Two field experiments are reported herein to evaluate the utility of electrical resistance tomography (ERT) for detecting and locating leaks as well as delineating any resulting plumes emanating from steel underground storage tanks (UST).

Current leak detection methods for single shell tanks require careful inventory monitoring, usually from liquid level sensors within the tank, or placement of chemical sensors in the soil under and around the tank. Liquid level sensors can signal a leak but are limited in sensitivity and, of course, give no information about the location or the leak or the distribution of the resulting plume. External sensors are expensive to retrofit and must be very densely spaced to assure reliable detection, especially in heterogeneous soils. The rational for using subsurface tomography is that it may have none of these shortcomings.

The strategy of our approach as shown in Figure 1 is, in a field demonstration, to produce a tomograph of electrical resistivity under a storage tank and look for changes in the subsurface resistivity which could be attributed to movement of the tank contents in the subsurface soil or groundwater. A straightforward approach to this task is to produce a tomograph of the soil under a tank and then, while observing the subsurface electrical properties, release the contaminant near the tank to simulate a leak. Unfortunately, this approach is not possible because laws protecting the environment prohibit intentional contamination even for research and development. Fortunately, the objectives of such research can be achieved by performing the work in two stages. For this reason the work described herein has been done in two parts. The first part of the work is to demonstrate that useful ERT images can be constructed in the soil beneath a large steel tank. The technical objective of this part is to produce images under a tank even when electrical currents are shunted away from the soil through the steel tank bottom. The second experiment is performed to determine if a common liquid stored in tanks, gasoline, can be detected in the subsurface using ERT. The technical objective of this part is to determine if an electrically resistive liquid, floating on the groundwater, could be detected using electrical methods.

2. Experimental Approach-tank leak detection

The first phase is to demonstrate that useful ERT images can be constructed for the soil beneath a large steel tank. The field experiment was performed under a 15 m diameter steel tank mockup (the tank was not actually used for liquid storage). About 4000 liters of 0.08 molar sodium chloride solution were released along a portion of the tank's edge to simulate a leak from "bathtub ring" corrosion. The release rate averaged about 26 liters/hour. Figure 2 shows the layout of the site where the experiments were performed.

ERT images were made before, during and after the brine release in each of 8 horizontal planes beneath the tank. Plane 8 is a cross section at the ground surface 1.5 m above the bottom of the tank (so it contained the tank itself). Plane 7 is 1.5 m lower, a cross section level with the tank bottom. Plane 6 is 1.5 m below the tank bottom and so on to plane 1 which is 10.7 m below the ground surface. This arrangement provided a series of image planes at many levels which, when assembled together, gave an overall view of the plume formed beneath the tank during the release and which could be used to determine the effects of imaging current shunted through the tank bottom.

Data was taken in each plane before the release and then repeated for each plane at several times during and after the release. To simulate the situation of a long term monitoring of a tank, we compared each data set taken during the release with that at a corresponding depth taken before the release. Two types of comparison were used. The first comparison was done by a pixel by pixel subtraction of images made from data taken before and during the release. The second comparison was done by inverting the quantity

$$\frac{R_a}{R_b} R_h$$

where R_a is the transfer resistance taken after the release, R_b is the transfer resistance taken before the release and R_h is the transfer resistance for the case where the resistivity is homogeneous. The transfer resistance is simply the ratio of voltage to current for an individual 4 electrode measurement. This comparison is a simplified perturbation from the uniform resistivity case as described in [2]. Other details of the data collection and inversion schemes are described by [2] and [3].

3. Experimental Results-tank leak detection

Figure 3 presents a series of two-dimensional tomographs collected from each electrode array at a given depth during the course of the release. The results show what areas of the soil changed in response to the brine spill. Each column of images shows the changes detected for a given time at various depths; the depth of images on each column increases from top (o m depth) to bottom (10.7 m depth). Time and leaked volume increase from left to right on the figure.

The images for July 26 at depths of 3 and 4.5 m (the top two available images of the first column in Figure 3; the top two planes were not collected at this time) show clearly detectable electrical conductivity increases directly below the release point. Note that the changes observed increase in magnitude as time and spilled volume increase. Also, note that the bottom of the changing region extends deeper as time increases. Electrical noise measurements were also made during the tests. These measurements where then used to calculate images which showed the magnitude of changes expected from measurement error (these error images are not shown). The resistivity changes shown in Figure 3 are substantially larger than those changes caused by measurement error. These observations support our conclusion that the changes observed are caused by the released brine as it invades the soil and not by some other unrelated phenomena such as measurement errors.

Although there is no cooberating data the images are consistent with the behavior expected for infiltration of salt water released into unsaturated soil. There is a clear decrease in resistivity of the volume directly below the release point. Furthermore, the changes are real and not the result of measurement error. The approximate leak location can be found directly above the region of maximum change on the top few planes. The lateral and vertical extent of the plume as a function of time can also be estimated from the images.

4. Experimental Approach-gasoline plume imaging

The purpose of this phase was to determine if ERT could be used to image the location and extent of free product gasoline in the subsurface. This work was performed at the Oregon Graduate Institute of Science and Technology (OGI) in Beaverton, Oregon because the facilities there include a unique double-wall tank filled with soil into which a contaminant could be released. The 10 m square and 5 m deep tank is instrumented for geophysical and hydrological studies. Sandy silt from river bottom sediments was randomly put into the tank; no effort was made to produce a structured fill (e.g., layers). The water table was controlled as needed, using city water having a 0.004 S/m conductivity. This facility makes possible a legal release of a hazardous contaminant into a soil at a scale sufficiently large to see real-world physical phenomena. A more complete description of the OGI facility can be found in [4].

Two boreholes in the tank were instrumented with electrodes and electrodes were installed on the surface between these holes. The reconstruction model assumes the resistivity distribution constant in the direction perpendicular to the plane defined by the electrodes although electrical potential is modeled three dimensionally to permit point source electrodes. The soil-air interface is a boundary of no normal current flow. After reconstruction, the tomographs are spatially smoothed to give the appearance of a continuous resistivity distribution. This, of course, doesn't improve resolution which can be no better than one mesh element. The mesh elements were approximately square and there were two elements between each electrode along the boreholes.

5. Experimental Results-gasoline plume imaging

A total of 408 liters of unleaded gasoline were released over an 81 hour period from August 28 through 31, 1992. This amounted to a rate of about 4 l/hr and was from a single point on the surface midway between the borholes. The phreatic surface, after being lowered from the soil surface, was stable at a depth of 80 cm for several days before the release (the vadose zone had drained from saturated condition during these several days).

ERT data were taken before, several times during and again after the release. The data taken before the release were the intended baseline but were particularly noisy. Several artifacts appeared in the image especially at the electrode positions. Because of these errors, we found the 'before' image to be unsuitable as a baseline. The data taken after the release of only 40 liters of gasoline had much less noise and was used as the baseline for the release sequence.

Figure 4 shows this August 28 baseline and subsequent pixel by pixel difference images. As early as August 30 we notice a definite resistive anomaly formed directly below the release point. It appears as a narrow anomaly from the surface downward and points to a larger anomaly which may be the main body of the plume at about the level of the original water saturated surface. The small anomaly pointed downward from the surface release point may be the barely resolved conduit from the surface to the point where the gasoline begins to spread in the capillary fringe. Such conduits are a common feature of large volume releases over short times and are called the descent cone by Farmer [5]. The larger anomaly below this descent cone is a 15 - 20 percent increase in resistivity over the background values which is larger than anomalies caused by measurement error. We believe this resistive anomaly is caused by gasoline accumulation in the available vadose porosity in the vicinity of the water table.

The main anomaly on August 30, September 1 and September 2 is centered on the original water table. Because gasoline will float on or near the top of the capillary fringe, its influence should be confined predominately to the upper portion of the saturated zone. However, if the gasoline only displaces pore air in this water-wet system, one resistive fluid replaces another, and this should not significantly change the net resistivity. Any perturbation of electric current flow in the partially saturated soil must result from either a spatial redistribution of the water or a change in the electrical properties of the pendular water (that held by capillarity).

The mechanisms for either of these conditions are not clear. One possibility is dissolved gasoline in the capillary water which should increase the bulk resistivity. However, solubility is so low that this effect can not account for the magnitude of the anomaly. (Samples of pore water with and without the dissolved gasoline was found to have the same resistivity within measurement error.)

Another possibility is a displacement of the capillary water by increased hydrostatic pressure as a result of replacing the air with gasoline. This might result in displacement of pendular water to cause the observed resistive anomaly. Perhaps a more likely mechanism is a change in the capillary suction of water arising from the introduction of gasoline into the pore volume. This mechanism requires that the pendular water capillary suction change as a result of replacement of the air-water interface in the partially saturated pore with a hydrocarbon-water interface. Such a change in capillary suction would mean a redistribution of pore water with a subsequent change in electrical properties. Whatever the mechanism, we believe that the hydrocarbon caused a net dewatering of the regions where gasoline entered the pore volume.

When the hydrocarbon reaches the capillary fringe, the relative permeability to the immiscible liquid declines and there is a tendency for lateral movement along the top of the fringe. Domenico and Schwartz [6] state that when a large volume of fluid reaches this point in a short time, the capillary fringe collapses (water drains under gravity to the fully saturated zone) and depresses the water table. They point out that the amount of depression depends on the quantity of product and its density but the fluid spreads in a relatively thin layer in the upper part of the capillary fringe. On the other hand, the ERT images imply a depressed water table and a relatively thick product layer. The anomaly appears in both the unsaturated and previously saturated portions of the soil. As described above, the mechanism for the electrical anomaly is probably displacement of pore water in both cases. Where the soil is water saturated, the gasoline with a specific gravity of 0.68, sinks to a level where buoyancy supports the mass. This displacement of water produced a resistive anomaly below the original water level.

On September 1 the anomaly appears larger in size and exhibits greater electrical contrast. No additional gasoline was released between the September 1 and September 2 images. The anomaly had not changed size on September 2 although there is evidence that it became more uniform and lower in overall contrast. This may be evidence of lateral spreading.

If the resistive anomaly represents the extent of a compact and continuous mass (say a volume 0.5 m thick and 2 m square using the September 1 image) in a soil of 20 percent available porosity (another assumption), we get a rough estimate of the released volume of gasoline at the end of the release of 400 liters. Although this is a simple analysis based on crude assumptions, the results compares favorably with the 408 liters released.

6. Summary and Conclusions

The work described above has been done to determine the feasibility of using ERT to detect and locate hydrocarbon leaks from large steel surface storage tanks. The strategy is to produce an ERT image under a tank and look for changes in subsurface resistivity arising from leaks as a plume moves through the soil. A tomographic image beneath a tank can be constructed with data from a relatively few electrodes at or near the ground surface yet each of the many pixels in that image acts as a separate leak sensor beneath the tank.

Many of the tanks in question are steel construction and contain hydrocarbon products. These facts define two principal issues requiring investigation. First can useful ERT images be made near a highly conducting steel tank bottom or will all the current used for imaging be shunted through the steel making in impossible to image the soil under the tank? Second, will an electrically insulating hydrocarbon produce a change in subsurface resistivity in the vadose or saturated soil which can be imaged by ERT? These issues had to be addressed separately because of laws prohibiting the release of hydrocarbon into the ground.

In one experiment we demonstrate that useful images of changes in electrical resistivity can be produced near the bottom of a large steel tank. This is accomplished by inverting a normalized ratio of data taken before and after a tracer release. Subsequent images delineate clearly the released tracer in reconstruction planes as close as a few meters from the tank bottom. However, a hydrocarbon plume will result in a lower electrical contrast than that produced by the salt water tracer used for the demonstration. Also we have not addressed complications such as cathodic protection systems used on tanks or natural subsurface seasonal variations. These effects will be studied in future work.

In another experiment we have demonstrated that a common tank constituent, gasoline, will produce a change in subsurface resistivity which can be electrically imaged. Results suggest that an optimal case for electrical detection is when the hydrocarbon depresses the capillary fringe at the water table. However, we have little evidence for how the method would work in a completely unsaturated soil. Results from the controlled gasoline imaging would also likely be much different in a geologically complex environment.

These two experiments suggest that it may be possible to detect and locate leaks in tanks using ERT. While the work demonstrates feasibility of the technique under the ideal, controlled circumstances available in these experiments, it does not prove that technique practical under more realistic conditions. Our work is continuing with the goal of studying the more realistic conditions caused by cathodic protection systems, infiltration of rain water, seasonal variation in the subsurface resistivity, contaminant type, variations in soil type, water table proximity, etc.

Acknowledgments

This study is based on work performed under the auspices of the U. S. Department of Energy by the Lawrence Livermore National Laboratory under contract W-7405-ENG-48.

References

[1] Cohen, R. M. and J. W. Mercer, *DNAPL Site Evaluation,* C. K. Smoley, 1993.

[2] Daily, W., A. Ramirez, D. LaBrecque and J. Natio, Electrical Resistivity Tomography of Vadose Water Movement, *Water Resources Research, 28,*1429-1442, 1992.

[3] LaBrecque, D. J., William Daily, Earle Owen and Abe Ramirez, Noise and OCCAM's Inversion of Resistivity Tomography Data,*Geopohysics,* in press, 1995.

[4] Johnson, R. L., Bagby, W., Perrott, M., and Chen, C. (1992). Experimental Examination of Integrated Soil Vapor Extraction Techniques, abst., *Proceedings of the 1992 Petroleum Hydrocarbons and Organic Chemicals in Ground Water: Prevention, Detection and Restoration,* November 4-6, Houston, TX.

[5] Farmer, V. E.(1983). Behavior of Petroleum Contaminants in an Underground Environment, Seminar on Groundwater and Petroleum Hydrocarbons, Protection, Detection, Restoration, *Proc. Petroleum Assoc. for Conservation of the Canadian Environment,* Ottawa.

[6] Domenico, P. A. and Schwartz, F. W. (1990). *Physical and Chemical Hydrogeology,* John Wiley, New York.

Figure Captions

Figure 1. Schematic of leak detection concept using ERT.

Figure 2. Schematic of experimental set up for leak detection. A 15 m diameter empty steel tank, the lower 2 meters of which is buried, contains a built-in spill point. Sixteen boreholes with eight electrodes in each surround the tank.

Figure 3. A series of two-dimensional ERT tomographs which show how the electrical conductivity of the soil increased during the side release experiment. Red colors indicate which portions of the images remain unchanged. Colors to the left of red indicate which portions of the image show electrical conductivity increases associated with the leak.

Figure 4. ERT 'baseline' taken on August 28 and difference images recorded during the gasoline release. The scale for the baseline image is shown at the top of the color bar and that for the other images is at the bottom.

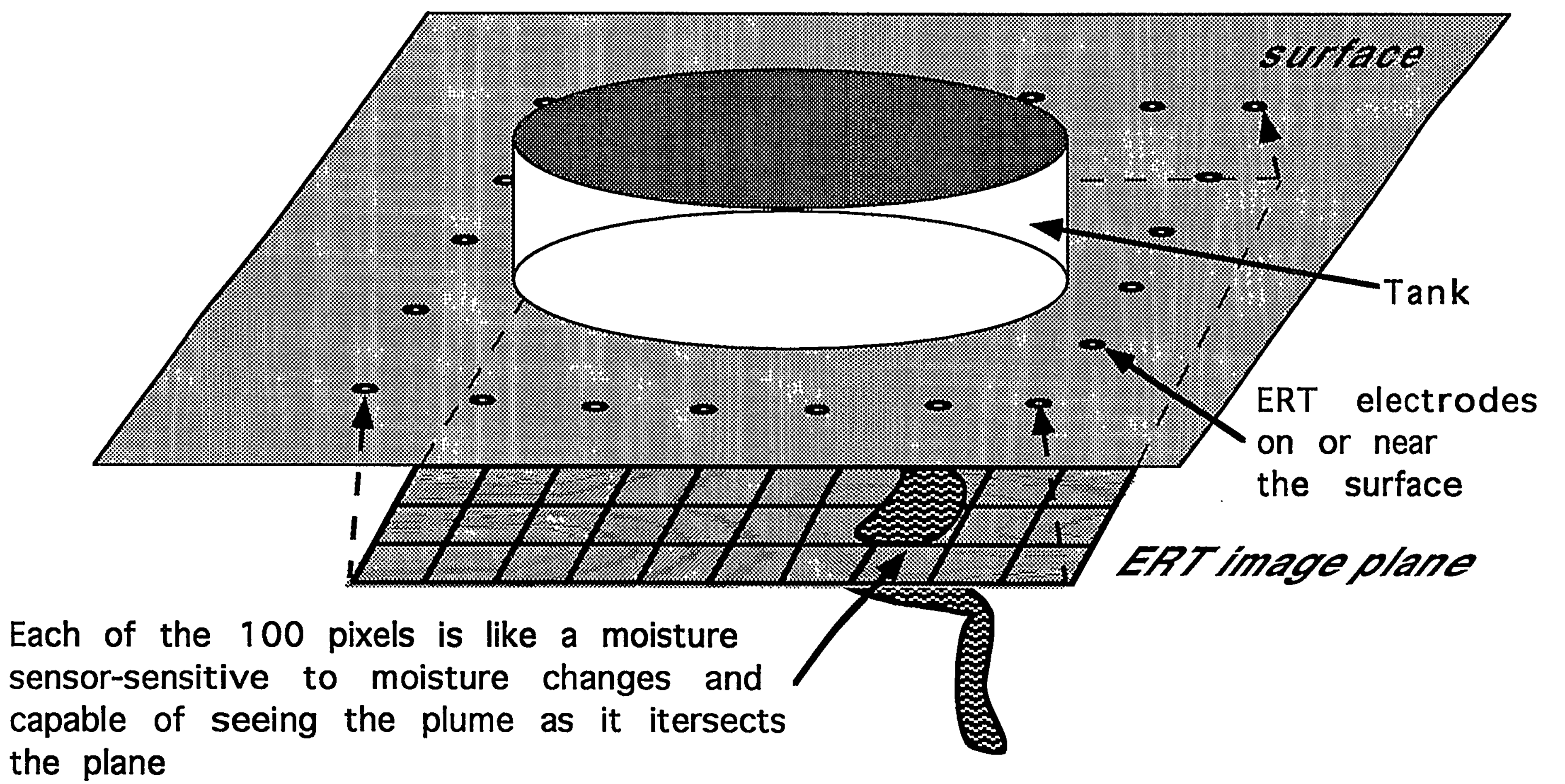
surface
Tank
ERT electrodes
on or near
the surface
ERT image plane
Each of the 100 pixels is like a moisture
sensor-sensitive to moisture changes and
capable of seeing the plume as it itersects
the plane

Fig. 1

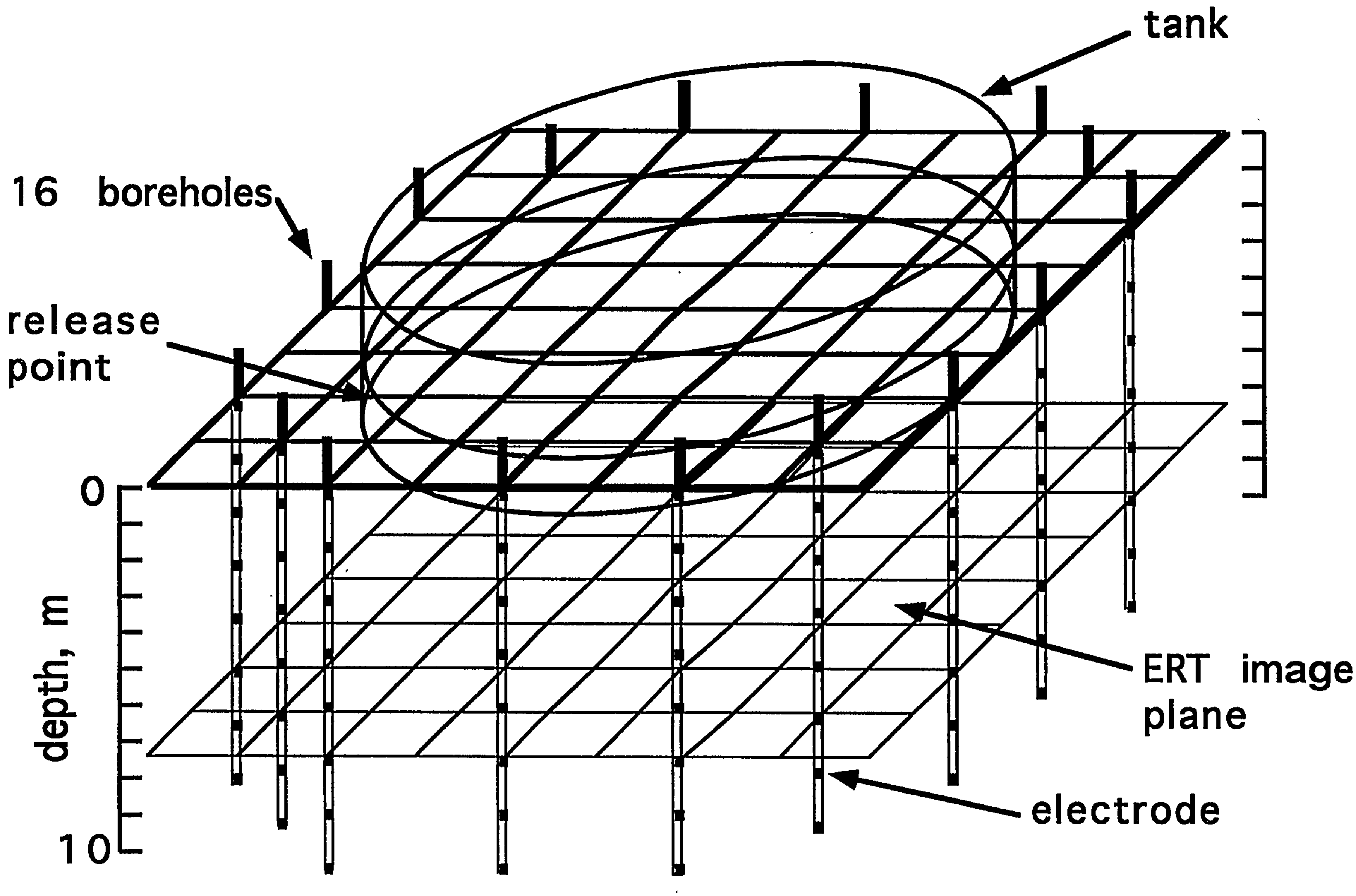
tank
16 boreholes
release point
0
depth, m
10
ERT image plane
electrode

Fig 2.

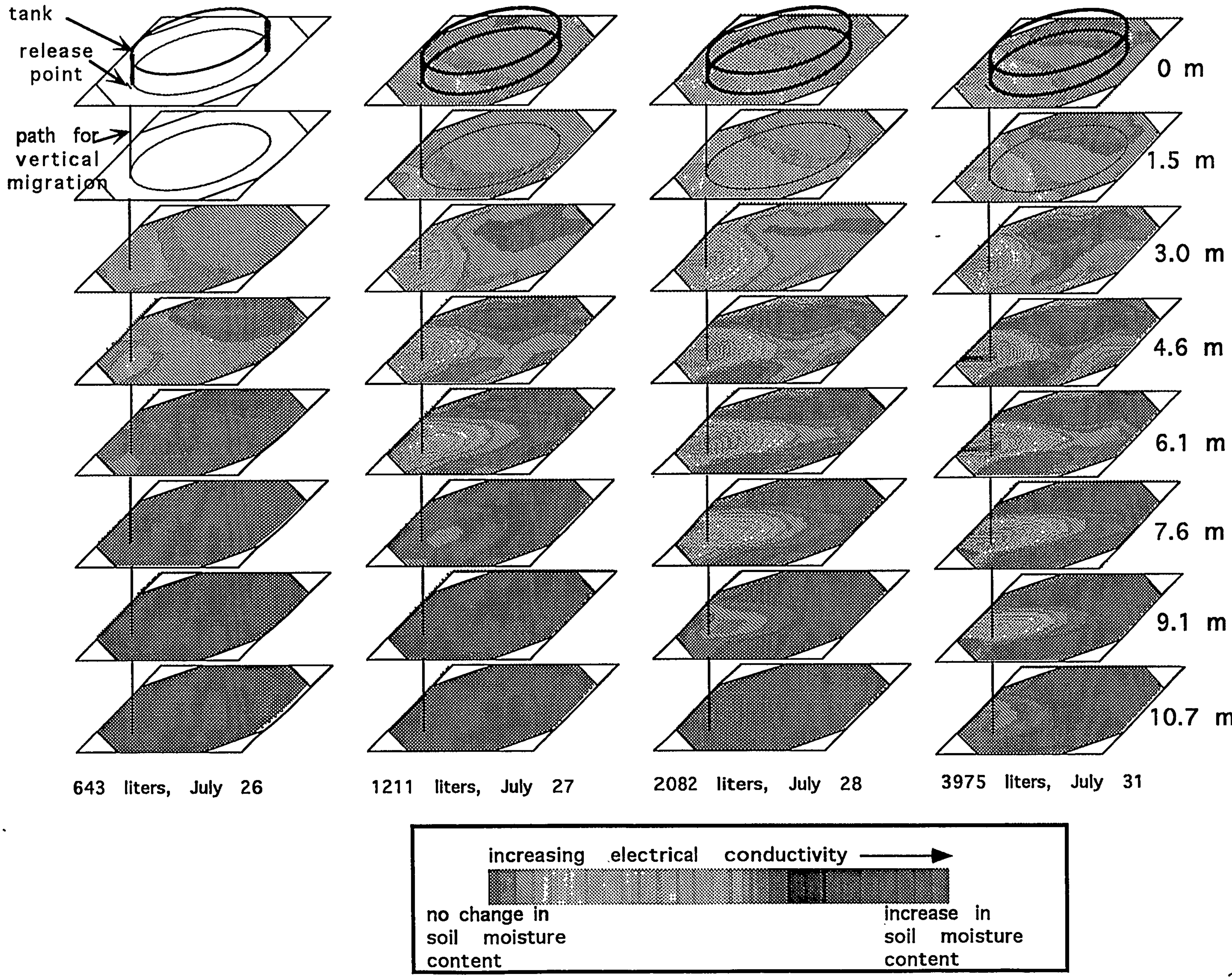
tank
release point
path for vertical migration
0 m
1.5 m
3.0 m
4.6 m
6.1 m
7.6 m
9.1 m
10.7 m
643 liters, July 26
1211 liters, July 27
2082 liters, July 28
3975 liters, July 31
increasing electrical conductivity
no change in soil moisture content
increase in soil moisture content

Fig. 3

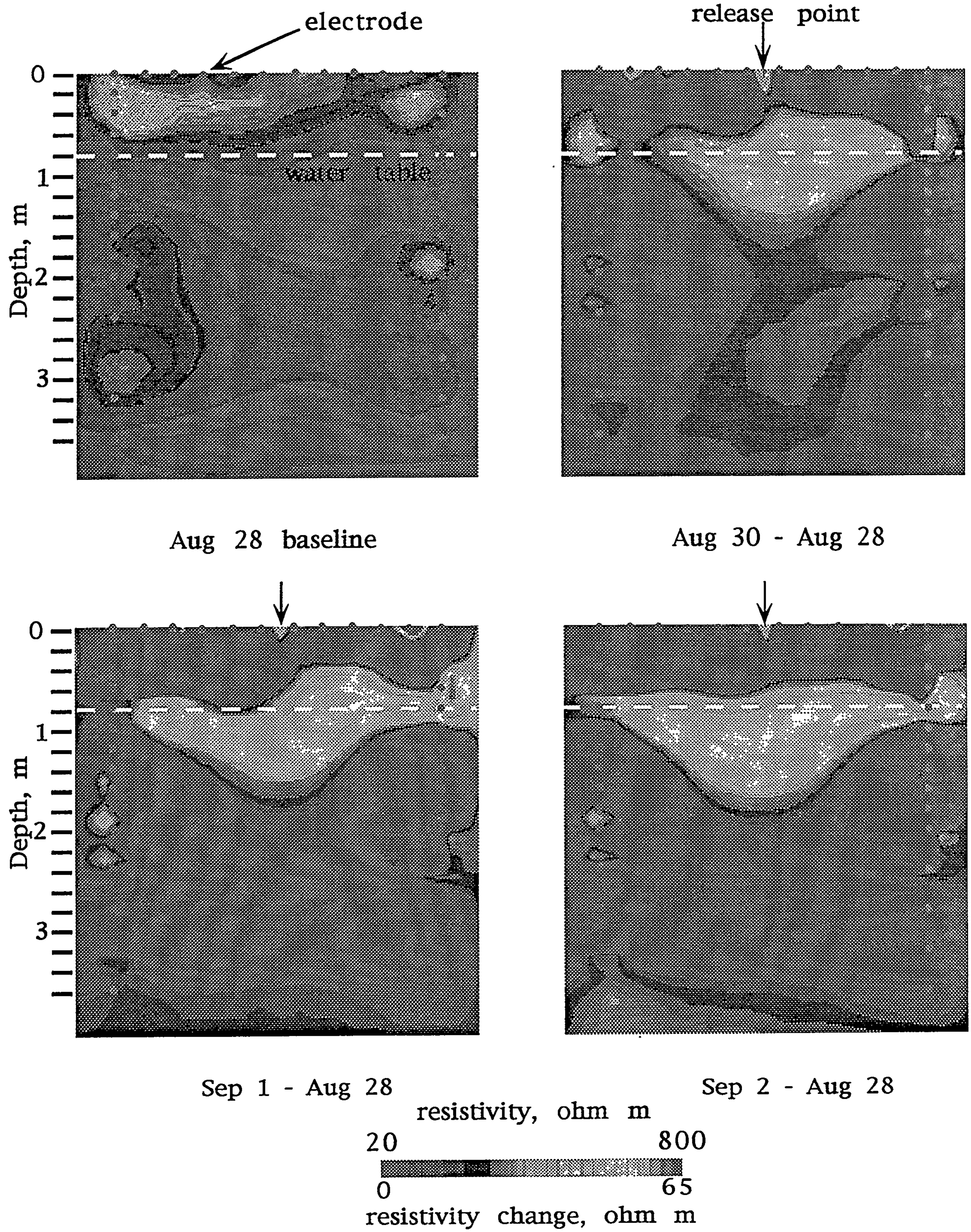
electrode
release point
0
1
2
3
Depth, m
water table
Aug 28 baseline
Aug 30 - Aug 28
Sep 1 - Aug 28
Sep 2 - Aug 28
resistivity, ohm m
20
800
0
65
resistivity change, ohm m

Fig. 4